Alifmatika: Jurnal Pendidikan dan Pembelajaran Matematika
Volume 5, Issue 2, 226-246, December 2023
e-ISSN: 2715-6109 | p-ISSN: 2715-6095
https://journal.ibrahimy.ac.id/index.php/Alifmatika

Cohen's kappa curves, new geometrical forms of dual curves

Laith H. M. Al-ossmi[1*], Imad Ibrahim Dawood[2]

[1*]College of Engineering, Thi-qar University, Al-Nasiriya City 370001, Iraq
[2]Mazaya University College, Al-Nasiriya City 370001, Iraq
[1*]laith-h@utq.edu.iq, [1*]hardmanquanny@gmail.com, [2]prof.dr.imad.i.dawood@mpu.edu.iq

Received: August 24, 2023 | Revised: October 22, 2023 | Accepted: November 15, 2023 | Published: December 15, 2023
*Corresponding author

Abstract:
In this article, we introduce the concepts of taxicab and uniform products in the context of dual curves associated with Cohen's kappa, primarily defined by a set of inflection curvatures of an ellipse and a circle using parallel asymptotes. The novel curve under scrutiny, denominated as the "Like-Bulb Filament" (LBF) curve, is delineated as the locus of dual vertices originating from a couple of conic curvatures. The emergence of LBF transpires through the orchestrated arrangement of line segments emanating from a predetermined central focal point upon an elliptical form concomitant with a circular entity possessing a radius equivalent to the ellipse's minor axis. The LBF's curve is intricately choreographed through the dynamic interplay of a constant unit circle and three asymptotic lines. Notably, two of these asymptotes achieve tangential intersections with the LBF curve, while the third gracefully traverses its central core. Additionally, we embark on a comprehensive algebraic examination complemented by a geometrically informed construction methodology. In these instances, a consistent conic curvature of the uint circle and an elliptical structure assume pivotal roles in the genesis of the LBF's curve. Also, a geometric connection is speculated between these curve configurations and their relevance to engineering processes across fields. However, the document acknowledges the need for more intensive study on the presented traits. Hence, it emphasizes addressing the existing research gap in subsequent investigations.

Keywords: Cohen's Kappa; Dual Curves; Geometric Methods; Nodal Curves.

How to Cite: Al-ossmi, L. H. M., & Dawood, I. I. (2023). Cohen's kappa curves, new geometrical forms of dual curves. *Alifmatika: Jurnal Pendidikan dan Pembelajaran Matematika*, 5(2), 226-246. https://doi.org/10.35316/alifmatika.2023.v5i2.226-246

Introduction

From a geometric perspective, a variety of 2D curves are constructed using geometric methods, where points are generated and connected with lines to define the curve's shape and points. Among these, a class of curves is known for their symmetry, derived from pairs of symmetrical curves along the horizontal or vertical axes. Notable examples of such symmetric curves include the Bullet-nose curve (Hašek, 2020), Kampyle of Eudoxus (Miura et al., 2022), Butterfly curve (Yücesan & Tükel, 2020), Atriphtaloid Sushanta (Ghuku & Saha, 2019; Saha, 2019), and the Kappa curve studied by Karkucinska-Wieckowska et al. (2022). These node-like and dual curves have garnered significant attention from researchers due to their intriguing characteristics (Gilani et al., 2020).

Specifically, the Kappa curve is a two-dimensional algebraic curve featuring three

inflection points and is also referred to as Gutschoven's curve. It was initially studied by G. van Gutschoven around 1662 (Findlen, 2011; Hašek, 2020), with subsequent investigations conducted by luminaries such as Isaac Newton (Gilani et al., 2020; Mary & Brouhard, 2019) and Johann Bernoulli (Yücesan & Tükel, 2020), who further delved into its properties.

Geometrically, this form of a class of dual curves exhibits two vertical asymptotes and maintains a clear symmetric profile along the y-axis, as well as the research conducted by Chan et al. (2021) and Miura et al. (2022). It is worth noting that the theory of curves holds a fundamental position within the realm of differential geometry. Characterizations of dual curves and dual focal curves have been explored within the context of dual Lorentzian space (Hašek, 2020; Magnaghi-Delfino & Norando, 2020) and have been applied to the study of isoptics of ovals, such as the Blaschke cylinder (Bobenko et al., 2020), as well as their related elliptical properties (Al-ossmi, 2023; Bialy, 2022).

Cohen's kappa coefficient, as depicted in Picture 1, which was noted, among others, by researchers such as Usman et al. (2020), is a statistic that is used to measure inter-rater reliability (and also intra-rater reliability) for qualitative (categorical) items. It is generally thought to be a more robust measure than simple percent agreement calculation, as κ takes into account the possibility of the agreement occurring by chance. Also, Cohen's kappa measures the agreement between two raters who each classify N items into C mutually exclusive categories (da Silva et al., 2020; Wang et al., 2021). According to Bialy (2022) and Yan et al. (2019), there is controversy surrounding Cohen's kappa due to the difficulty in interpreting agreement indices.

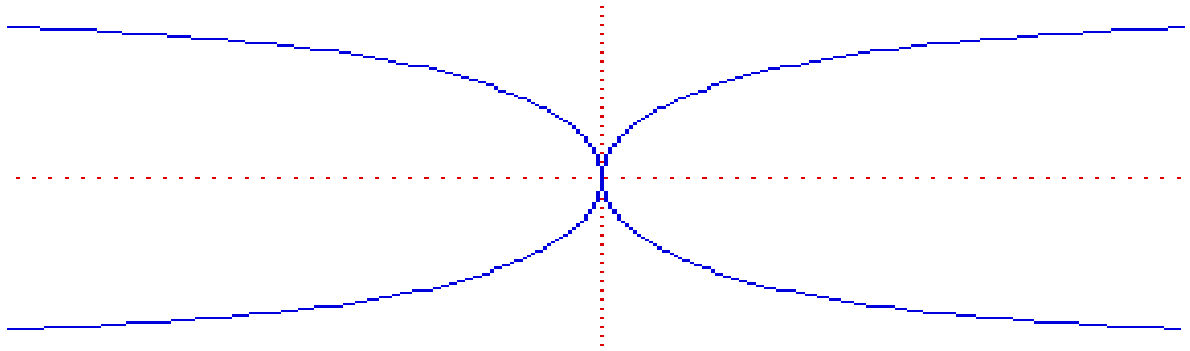

Picture 1. The H. Kappa's curve has two vertical asymptotes and An Atriphtaloid with $a = 3$ and $b = 2$ (Więckowska et al., 2022)

This article operates based on the premise that Cohen's kappa curves are unbounded in infinity along the ± x-axis. Therefore, it is possible to explore new curves stemming from this point. The study primarily focuses on generating cases of curves through the utilization of conic sections, specifically the pair consisting of the ellipse and the circle, where the minor and major axes of the ellipse are varied. Through this approach, the research produces two novel instances of curves, which are examined within the scope of this article.

The article focuses on studying new characteristics of Cohen's curve through the innovation of a geometric method for generating a new form of open and closed curves, specifically producing two significant special cases: a dual curve and a linear curve with an intersection point (cusp) within the circumference of the inscribed conic curvatures. These two generated cases represent the novel contributions of this article regarding

Cohen's curve, which has not been addressed in previous studies that only considered the typical form of the curve. The current study presents two geometric methods for drawing Cohen's curve in these new cases introduced to analyze the properties and distinctive features. It offers a straightforward characterization of dual atriphtal curves by means of the conic curvature inherent to a circle and an ellipse. In light of this research, the newly coined term "Trident" is introduced to designate this distinct curve, which is hereby denominated as "The Like-Bulb Filament" (LBF) curve. Consequently, this nomenclature is employed throughout the paper to reference this specific curve whenever it is encountered.

The article also does not delve into the statistical aspects of Cohen's curve, nor is it related to the correlation properties between the Cohen-Macaulay property of a projective monomial curve. Subsequently, the article undertakes an extensive study of Cohen's kappa curve, with the primary objective of its regeneration, resulting in a novel configuration of dual open curves. This reconfiguration is accomplished by amalgamating curvatures from a circle and an ellipse while focusing on the tangential intersection of two asymptotes with the LBF's curves. In contrast, the third asymptote traverses through the central region of the LBF's curves. Consequently, a new class of dual focal curves, embodied by the systematic and intricately structured LBF's curve within dual 2-space, is rigorously analyzed and visually represented.

Research Methods

This article introduces a novel category of the open form of Cohen Kopper's curves, referred to as LBF's nodal curves. The primary objective of this paper is to meticulously explore and dissect the unique characteristics of this LBF's curve, which is accomplished through the formulation of two distinct construction methods. The first method intricately involves using two tangent curvatures, specifically an ellipse and a circle, combined with asymptotes. The second equally precise method revolves around utilizing a circle and two horizontal asymptotes. In both methodologies, a specific point, denoted as (A), is meticulously positioned along the x-axis, its precise distance from the center of the fixed circle carefully measured as (a).

In both methods, the precise determination of any point residing on the LBF's curve is meticulously executed through a rigorously defined geometric procedure that relies on the exact intersections of lines meticulously emanating from a comment point. These lines were systematically oriented to intersect the upper and lower horizontal axes, which are tangent to the conic curvature of a circle with pinpoint accuracy (Lin & Yang, 2018; Liu, 2017; Simon Wedlund et al., 2022; Szubiakowski & Włodarczyk, 2018; Weil et al., 2013). This process is executed precisely, entailing a series of line segments meticulously extending from the curvature of a centered circle and ellipse in method (No. 1) or a set of parallel asymptotes, as geometrically tuned in method 2. Subsequently, perpendicular segments extend from these meticulously determined intersection points to intersect the x-axis. These segments then reflect at the same precise angle (u) to intersect the segment drawn from the ellipse at an exact point, where the angle (u) is varied via ($0 \geq u \leq \pi/2$). This comment point (A), with precise geometric coordinates of curvatures of a circle and an ellipse, and (u), are close parametric factors on the LBF's nodal curve.

In a comprehensive and precise context, this work also presents the concepts of taxicab and uniform products for this new dual form of Cohen's kappa, rigorously characterized by a precisely defined set of inflection curvatures and parallel asymptotes.

Also, all figures and obtained measurements provided in this paper are executed with the utmost precision using the Auto-CAD program, Version 2022, ensuring that each detail is meticulously accounted for.

Research Result

Properties of LBF's Constructing Method (No. 1)

This method (No. 1) is of a circle and two horizontal asymptotes; hence, LBF's curve in this method is generated through the utilization of a circular curvature and two parallel asymptotes. In Picture 2, this method is visually depicted, with point (A) situated at the base of the circle, coinciding with the origin point. It is worth noting that the resultant curve in this method comprises two symmetric components, each positioned on either side of the y-coordinate axis. The vertices of each curve are precisely aligned with the midline that passes through the center of the circumscribed circle ($y = a$). Furthermore, it is observable that each of the two curve segments consistently intersects the x-axis on both sides at a singular point denoted as (Bn), at a precise distance of ($3a$) from the center of the circle. These segments extend infinitely along the x-coordinate without intersecting with the asymptotes as they approach infinity (refer to Picture 2). To facilitate the plotting of the LBF's curve using the method involving a circle and two horizontal asymptotes, the following steps, as outlined in Picture 2, are imperative:

1. Let a circle with a radius of (a), where point (A) lies at the base of the circle and is positioned at the origin (x, y).
2. Construct two tangents extending from the upper and lowermost points of the circle, in which three parallel line segments as the asymptotes lie at ($y = 0$), ($y = a$), and finally ($y = 2a$).
3. Starting from point (A), draw a line segment (APn) that intersects the upper asymptote while passing through the circle.
4. Subsequently, by adhering to these preceding steps, as elucidated in Picture 3, the points that comprise LBF's curve are incrementally generated.

Additionally, Picture 2 outlines the application of this method in two cases, where the angle (u) is varied via ($0 \geq u \leq \pi/2$), and it is set to two different values. It specifies that 3 of LBF's asymptotes are directly correlated to the value of ($2a$); whenever the radius length of the circle is increased, the inflation points of the curve gradually increase, and the curve points at levels of ($y = a$) and ($y = 2a$) are proportionally increased too, as the value of ($2a$) is a leading parameter.

In this method, it can be noticed that a single curve lies symmetrically at each side of ± x-axis; hence, the vertex points of both sides of the LBF's curve, (±Bn), lies at a fixed distance of ($\pm 3a$) from the center point of the drawing circle. Also, this distance, ($3a$), is a constant in LBF's proportions as well as the position of a point (A), which is determined along both ± x-axis or y-axis; further studies would be useful to investigate this indication (Picture 2).

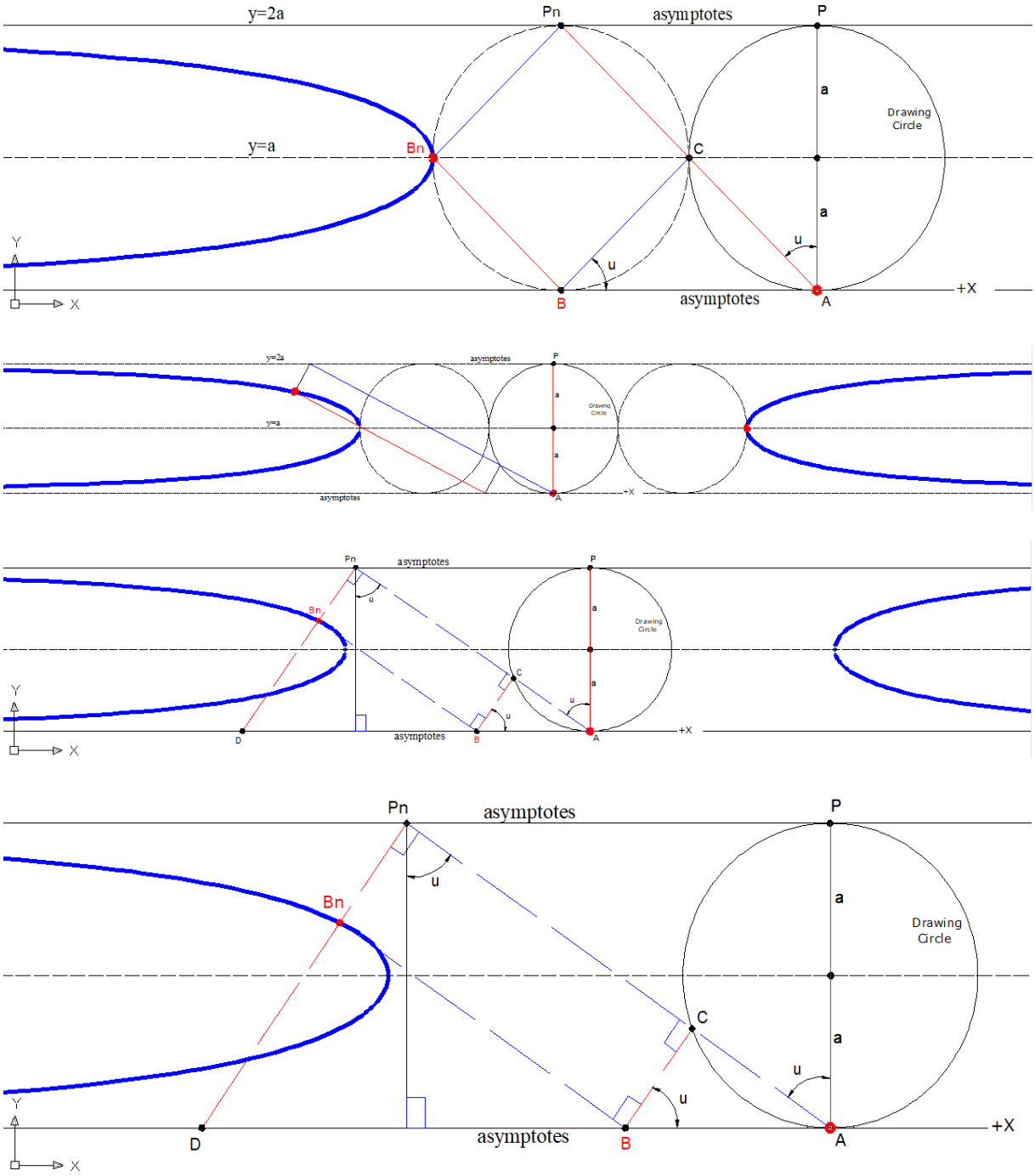

Picture 2. Plot a constructing method for LBF's curve (method of a circle and three horizontal asymptotes); hence, the LBF's curve is plotted by using 2 cases where $(0 \geq u \leq \pi/2)$

Additionally, it is noteworthy that another construction method (No. 1) for the LBF curve involves using a circle and two horizontal asymptotes. This method introduces a parameter, denoted as angle (u), where $(0 \geq u \leq \pi/2)$, which plays a crucial role in the construction process. It is anticipated that varying the angle (u) may lead to different characteristics and variations in the resulting LBF's curve. To gain a comprehensive understanding of the construction process and the outcomes associated with this method, it is imperative to delve into additional details and equations pertaining to the construction of LBFs.

In this context, the roles of both the angle (u) and the parameter (a) in this method (No. 1) are of paramount importance as they serve as leading factors in determining the geometric properties of LBF's curve in this method. A thorough exploration of these factors is instrumental in elucidating the geometric characteristics and intricacies of LBF's construction. Correspondingly, a single curve is drawn with a vertex point that intersects the drawing circle at $3a$ and passes through the x-axis, representing the axis of symmetry for the LBF's curve at ($y = a$). Furthermore, we note that the vertex point of the LBF's curve on both sides of the $\pm x$ is located at a constant distance equal to $\pm 3a$. The significance of angle (u) is that it is the varied parameter, while the drawing circle (a) radius is used as a leading constant in this method, in which the shape of LBF's curve is geometrically fixed. The LBF's angle (u) is a parameter likely affecting the shape or characteristics of the LBF curve. Meanwhile, this method describes the radius of the drawing circle (a) as a constant. It seems that this parameter (a) is a fundamental factor in determining the shape of the LBF curve. The geometric properties of the LBF curve are fixed based on the chosen constant value of (a).

Similarly, the key proportion of LBF shared with the Koppa curve is that both are extended into infinity (Picture 3). Nevertheless, the LBF's curve has three parallel asymptotes at ($y = 0$), ($y = $ a), and ($y = 2a$). Also, the LBF's curve shares a significant characteristic with the Koppa's curve, suggesting that both curves continue indefinitely without reaching a finite endpoint. Also, the LBF's curve is drawn by conic curvatures of a circle and ellipse, and it is described as having three parallel asymptotes; however, both curves extend towards infinity since they approach these horizontal lines without ever crossing them, Picture 2.

In Picture 3, the first case of the LBF's curve shifted by a curvature of the circle shares the same length of the drawing circle's radius (a), as they work as a set of curvatures along the x-axis. In this method (No. 1), suppose that point (A) is at the origin and placed on the x-axis. Then, LBF 's curve is constructed from (A). The parameters of (u) and (a) are the slope angle and radius of the drawing circle, respectively, leading parameters of the LBF's curve. It imparts geometric determinism to the LBF's curve, firmly anchoring its shape and character. The intricate interplay of these parameters governs the intricate geometric nuances of the LBF's curve. Upon meticulous examination of each point positioned along the x-axis of the ellipse, it becomes apparent that the resultant curves yield nodes that precisely align themselves with a distinct auxiliary ellipse. This intriguing observation underscores the intricate and enigmatic relationship shared between the LBF's curve and these ancillary curvatures, implying the existence of profound geometrical connections yet to be fully unveiled, as elucidated in Picture 3.

From point (A), extend a line segment to extend both the parallel asymptotes passing through the drawing circle at (An) and the asymptotes (P). then construct a perpendicular from point (An) to intersect the x-axis at (D), then draw (AnD), then from (D) draw a line segment (PB) which is parallax and equal to (DAn), then link from (D) to (B) where (BD) = (Pan), Picture 3.

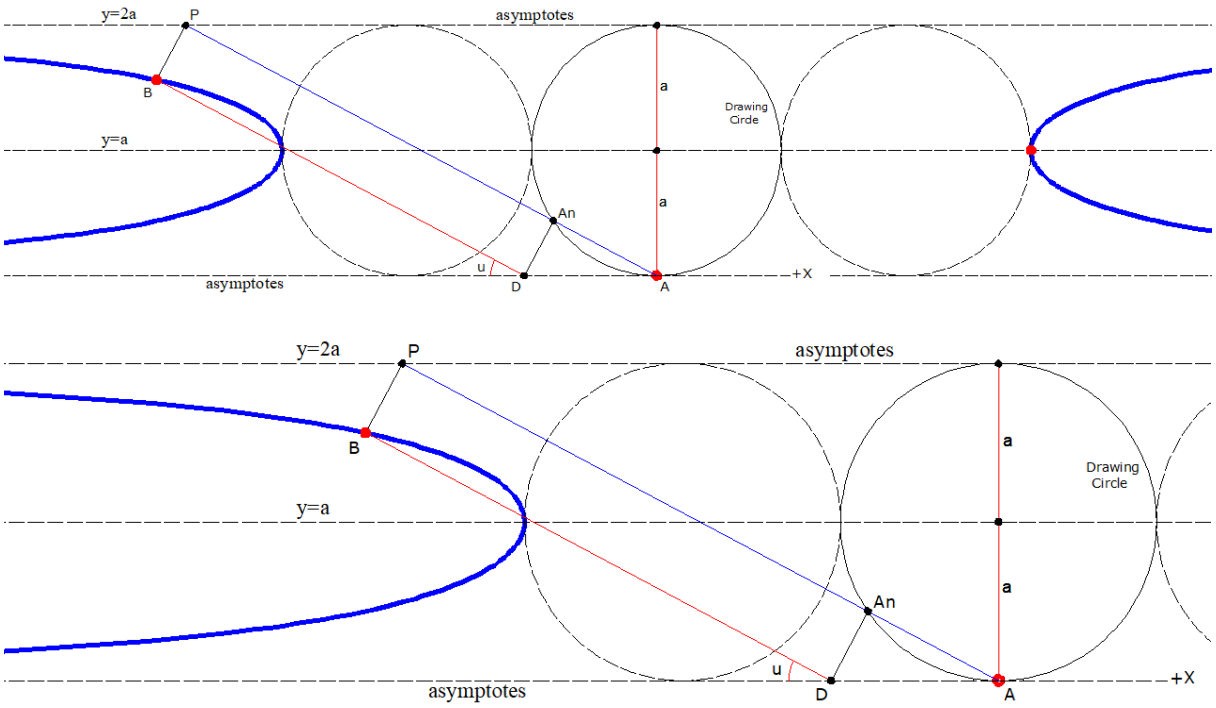

Picture 3. Plotting the geometric method (No. 1) to determine the LBF's curve points, (B), where (a) and (u) are LBF's parameters.

In this method (No. 1), both (a) and (u) are LBF's parameters. From the right-angled triangle ($DAnA$), and according to the LBF's properties, the line segments (AnA) and (PA) are parallel; then we can find LBF's Cartesian equation as follows;

$$AnA = 2a\,cos(90 - u), \tag{1}$$

$$PA = 2a/\,sin\,u, \tag{2}$$

Then, the length of the line segments (DB) and (DA) can be determined by;

$$BD = \left(\left(\frac{2a}{sin\,u}\right) - 2a\,cos(90 - u)\right), \tag{3}$$

$$DA = \left(\frac{2a\,cos(90 - u)\,.\,tan\,u}{sin\,u}\right), \tag{4}$$

Accordingly, the LBF's point (B) depends on the value of both line segment of (BD) and the perpendicular from point (B); therefore, the value of y and x of any point of the LBF can be obtained by;

$$\boldsymbol{y} = sin\,u\left(\left(\frac{2a}{sin\,u}\right) - 2a\,cos(90 - u)\right), \tag{5}$$

$$\boldsymbol{x} = cos\,u.\left(\left(\frac{2a}{sin\,u}\right) - 2a\,cos(90 - u)\right) + \left(\frac{2a\,cos(90 - u)\,.\,tan\,u}{sin\,u}\right), \tag{6}$$

It is an important point that the LBF's Cartesian equation of any point of the curve, B(x,y) can be determined by both parameters of (a) and (u); the segments of (AP) extend from the fixed point (A) along the third asymptote, ($y = 2a$), with an angle (u), where ($0 \geq u \leq \pi/2$), which play a crucial role in the LBF's construction process in Method (1). However, a special case of LBF's curve is produced in this Method (No.1), in which the LBF's curve has a duality form.

The duality of LBF 's Curve:

A special case of the duality of LBF 's curve is produced in this Method (No.1). This case is produced if point (A) lies on the circle center where each two asymptotes are located at a distance (a) from point (A) and parallel to the x-axis. The same geometrical steps are followed by drawing a set of line segments from (A) to intersect the circle circumference passing through the tangent asymptote. Then, by constructing a perpendicular from each previous intersection point (P) to intersect the x-axis at (An) and then from it paralleling to that ray drawn from (Pn), the intersection point (Bn) is a point of LBF 's curve, (Picture 4). Also, figures and the obtained measurements provided in Pictures 4 and 5 are executed with the utmost precision using the Auto-CAD program, Version 2022, ensuring that each detail is meticulously accounted for.

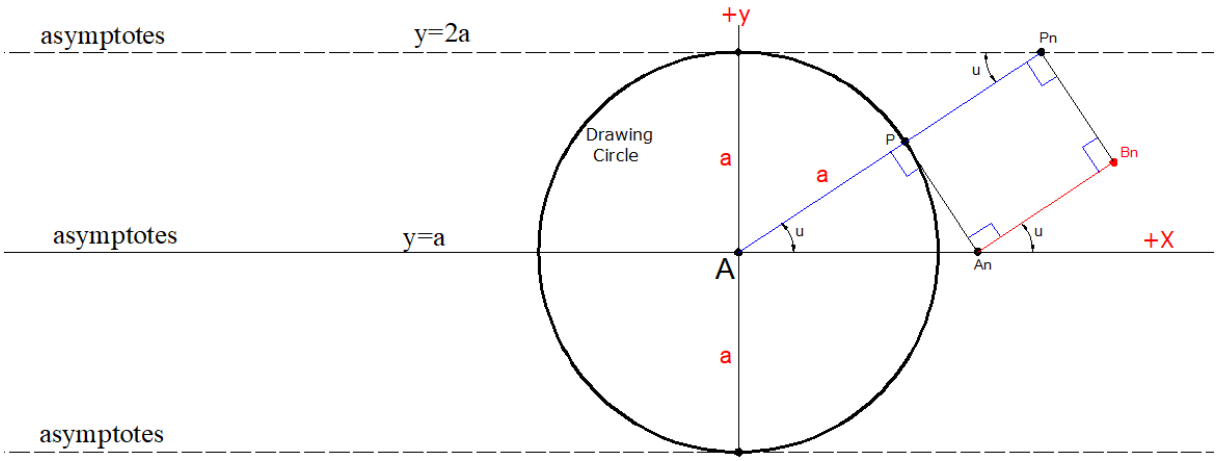

Picture 4. Polt the process of the duality of LBF 's curve produced in this Method (No.1)

In order to plot the duality of LBF 's curve using the method of a circle and three horizontal asymptotes, the following steps (in Picture 4) are required:

Let a circle with radius (a), where point (A) lies on the center point;

Construct two tangents from the top and bottom points of the circle, which are the asymptotes;

By angle (u) where ($0 \geq u \leq \pi/2$), then form point (A), construct a line segment (APn) to intersect the top asymptote at (Pn) and pass through the circle at (P);

Then, from point (P), draw a perpendicular to intersect the x-axis at (An), copy the segment (PAn) to be at (Pn) so that (PAn) = (PnB), and then (PPn)= (AnB).

Then, by following these previous steps illustrated in Pic.4, and for a useful timesaving tool, the Auto-CAD program, Version 2022, is used so that all points of LBF's curve are gradually produced, and a dual segment of LBF's curve is shaped along the ± x-axis, Picture 5.

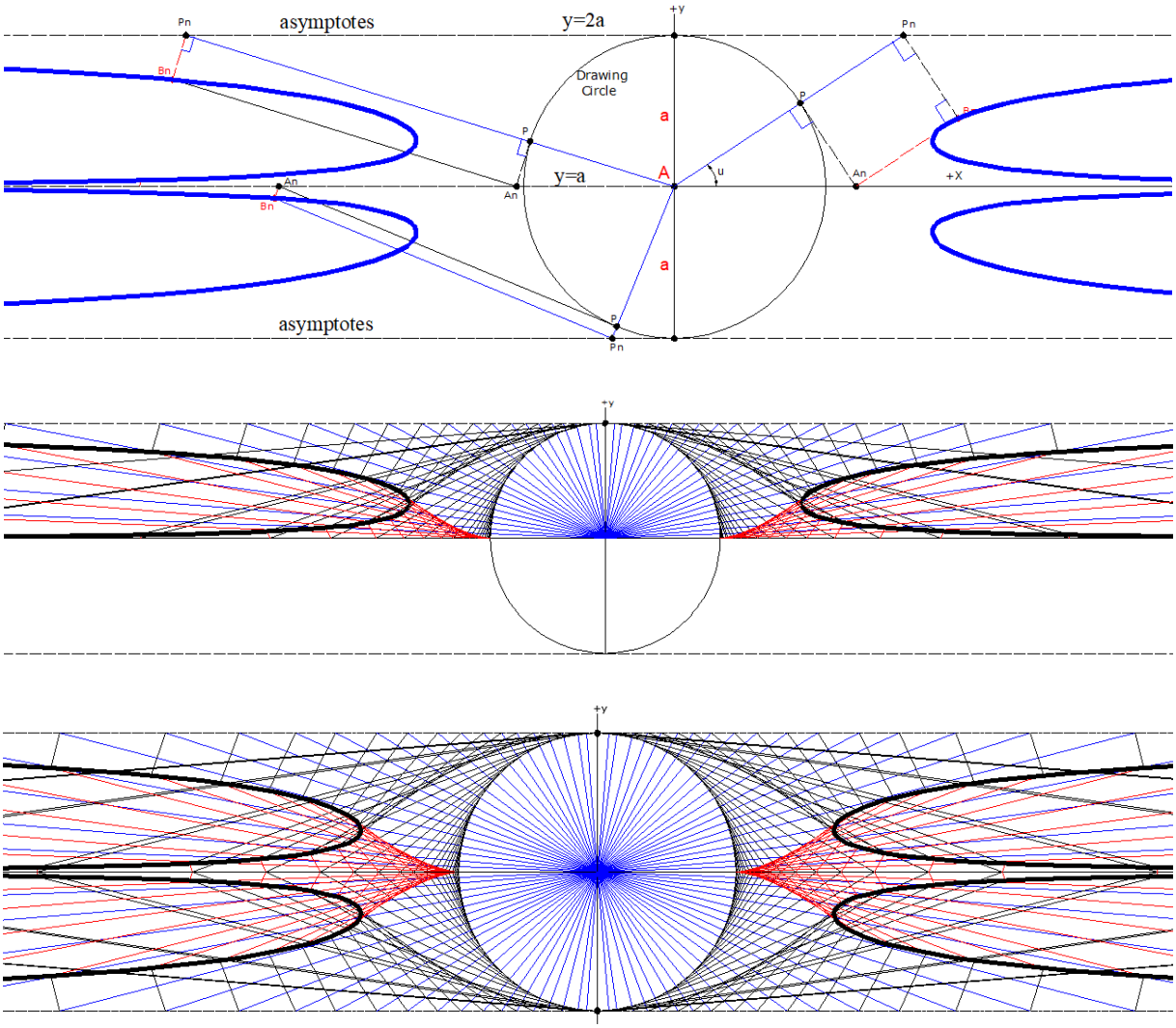

Picture 5. The dual LBF's curve, in this special case, is plotted by linking a set of rays from the drawing circle's point (A) to any asymptote, completing a full round of (2π).

Picture 5 shows that the LBF's curve in this special case in method (1) is produced with four nodal curves that parallel at the middle asymptote and pass infinity through the center point of the drawing circle. Similarly, it is noticeable that at each side of the drawing circle, the LBF's dual parts extend towards the tangent asymptote, while they closely extend to each other along the symmetry asymptote, which passes through the drawing circle's center, point (A). By completing a full round of (2π), there are a couple of intersection points in which the LBF's drawing circle intersects the ± x-axis since they can be used as the focus of both segments of the curve, due to through them all rays are intersected at the circle circumference at (a, ±a). The duality of the LBF's curve indicates that a circle and three asymptotes draw a special case; hence, each of the two segments of the curve extends along the ± x-axis in infinity, and they come close to the three asymptotes (y = 0), and (y = ±a), where ($0 \geq u \leq \pi/2$), as it is illustrated in Picture 6.

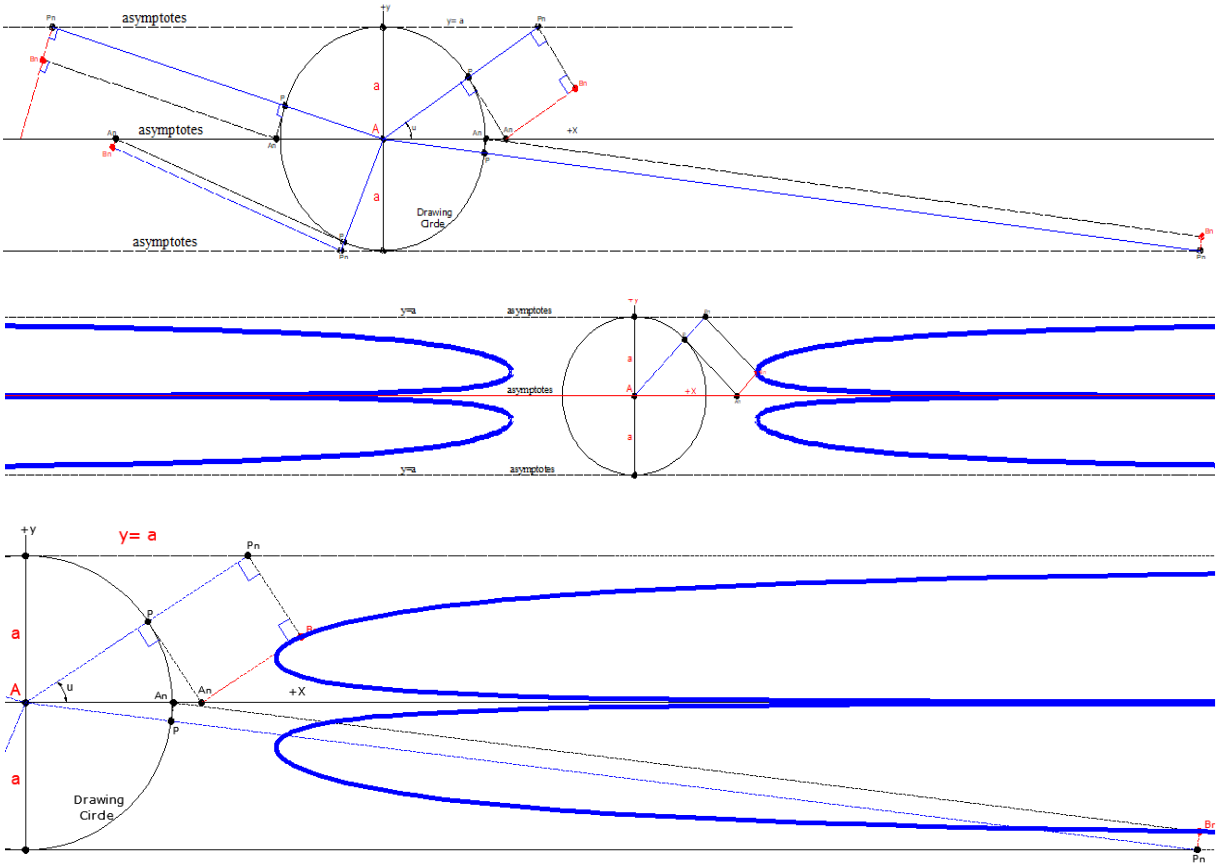

Picture 6. The dual LBF's curve, in this special case, is drawn by a circle and three asymptotes

Similarly, from Pictures 5 and 6, it is seen that whenever this ray (*APn*) completes from point (*A*) around (π/2), then a single segment of LBF's curve is produced. Thus, LBF's curve in this special case is plotting if the ray from point (*A*) to any asymptote at (*a*) is completing a full round (2π). The LBF's curve in all four segments extends in infinity along the three asymptotes. Point (*A*) at the center of the drawing circle is the focus of LBF's curve in this special case. Parametric equations of the LBF's curve in this special case can be produced as follows.

Let a drawing circle with a radius (*a*) and a center point (*A*), which tangent the x-axis at the origin point (0,0).

Construct three horizontal lines, ($y = 0$) and ($y = \pm a$); hence, two of them tangent the circle while the third passes through the center point (*A*). Then, construct a ray from (*A*) that passes through the circle and the asymptote at (*P*) and (*Pn*), respectively. Then, from point (*P*), draw a perpendicular at (*APn*), which intersects the x-axis at (*An*). From point (*Pn*), construct line segment (*PnBn*), which is parallel and equals the (*APn*). Then, link between (*An*) and (*Bn*) so that (*PnBn*) = (*PnP*).

From Picture 6, the triangle Δ (*APAn*) is right-angled, the line segments (*AnP*) and (*PA*) are parallel, and ($PA = a$), then we can find LBF's Cartesian equation in this special case as follows.

$$APn = \frac{a}{\sin u}, \tag{7}$$

$$PPn = \left(\frac{a}{\sin u} - a\right) = \frac{a(1-\sin u)}{\sin u}, \tag{8}$$

According to the LBF's proportions in Method (1), the line segments (*PPn*) = (*AnBn*), then;

$$PPn = AnBn = \frac{a(1-\sin u)}{\sin u}, \tag{9}$$

Then, from the right-angled triangle Δ(*AnBnyx*),
the value of *y* and *x* of any point of the LBF, (*Bn*), can be obtained by;

$$y = \frac{\cos u}{AnBn}, \tag{10}$$

$$x = \frac{\sin u}{AnBn}, \tag{11}$$

$$\boldsymbol{y} = \left(\frac{\sin u \,.\cos u}{a(1-\sin u)}\right), \tag{12}$$

Where the LBF's point is (*Bn*), the three asymptotes lie (y = 0) and (y = ±*a*), and angle u is ($0 \geq u \leq \pi/2$). Value of *x* can be obtained by adding the distance of Δ (*AAn*), which is obtained from the right-angled triangle (*APAn*), then;

$$\tan u = \frac{PAn}{AnBn},$$

$$PAn = \left(\frac{a(1-\sin u)}{\sin u}\right)\tan u, \tag{13}$$

$$\boldsymbol{x} = \left(\frac{a(1-\sin u)}{\sin u}\right)\tan u + \left(\frac{\sin^2 u}{a(1-\sin u)}\right), \tag{14}$$

LBF's Curve Constructing Method (No.2).

As mentioned, the LBF's cirve in this article is produced using two methods. The second constructing method uses two conic curvatures, an ellipse and a circle. This method (2) is built by a curvature of an ellipse sharing the same length of the minor axis (*a*) and the center point (*A*) with a circle. Also, in this method, the LBF's curve is constructed by a set of rays from the center point (*A*), extended to intersect the circumference of the circle and the ellipse at (*P*) and (*Pn*), respectively (see Picture 7). Generally, the same previous geometrical steps are used in this method; hence, the nodes at both sides of the center point (*A*) are parametrically according to the ratio of the ellipse axis (*a*) and (*b*) so that the curve intersects the end of the ellipse along the major axis which is here the symmetry axis along the x-axis, (Picture 7).

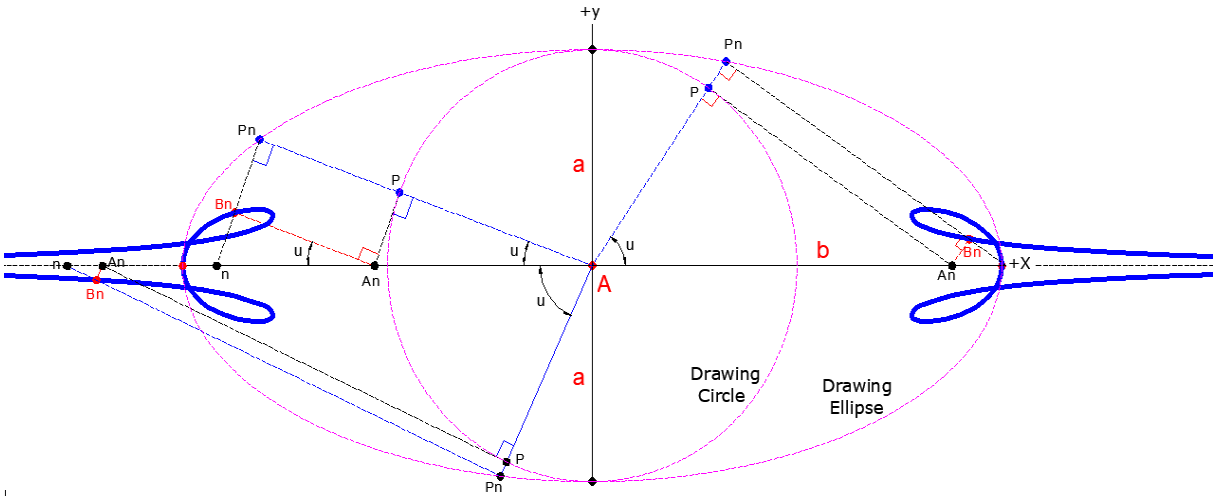

Picture 7. Plot the LBF's geometric properties according to the method (No.2)

In this connection, the same radius value of the drawing circle is (a), and their points share the same value of (y), whereas they differ by the value of (x). In the LBF's, it can be seen that the equation of (No. 2) gives a value of (x), which is precisely dependent on the drawing ellipse's major axis.

Therefore, the value of the drawing circle's radius (a) is equal to the minor axis of the ellipse, and angle (u) is varied over ($0 \geq u \leq \pi$); all are comparative parameters for both segments of LBF's curves drawn by this method (No. 2); hence the dual curves of LBF are extended in infinity along the positive and negative x-axis. Mathematically, LBF's curve in this method is constructed from a set of rays constructed from point (A) and both parameters of drawing curvatures, (a), (b), and angle (u) (Picture 7) from the right-angled triangle ($\Delta APAn$), and by using ellipse proportions, and simple trigonometry.

$$APn = \sqrt{a^2\left(1 - \frac{x^2}{b^2}\right)}, \tag{14}$$

$$PnP = AnBn = \sqrt{a^2\left(1 - \frac{x^2}{b^2}\right)} - a, \tag{15}$$

Thus, the value of y and x of any point of the LBF, (Bn), can be obtained by these equations;

$$\boldsymbol{y} = \sin u \left(\sqrt{a^2\left(1 - \frac{x^2}{b^2}\right)} - a\right), \tag{16}$$

$$\boldsymbol{x} = (b - \cos u)\left(\sqrt{a^2\left(1 - \frac{x^2}{b^2}\right)} - a\right), \tag{17}$$

Also, in this method, the single asymptote passes through the ellipse center point (A) at ($y = \pm a$), and angle u is ($0 \geq u \leq \pi$).

It is interesting to note that this kind of curve shows another remarkable fact. All dual nodes of the LBF's curve make up from each side a part of a minor ellipse whose

end point of its major axis is the intersection point of the curve at the x-axis; hence, the dual curves are extended in infinity along the positive and negative x-axis. At each point of the ellipse located at the *x*-axis, the curves produce a node that fits on a rather ellipse; also, the angle (u) values are varied within a range smaller than that in method (1). Similarly, in this method, it is seen that the minor axis, which is the radius of the drawing circle (*a*), is described as the highest value of the y-axis in this method. In contrast, the major axis's value determines the cusp shape inside the ellipse perimeter. It seems that parameters (*a*) and (*b*) are fundamental factors in determining the cusp shape of the LBF curve in this method. The geometric properties of the LBF curve in this method are fixed based on the chosen constant value of (a) (Picture 8). All these geometrical aspects need to be studied further. Thus, future studies may help to give further information about these geometrical relationships of LBF's curve.

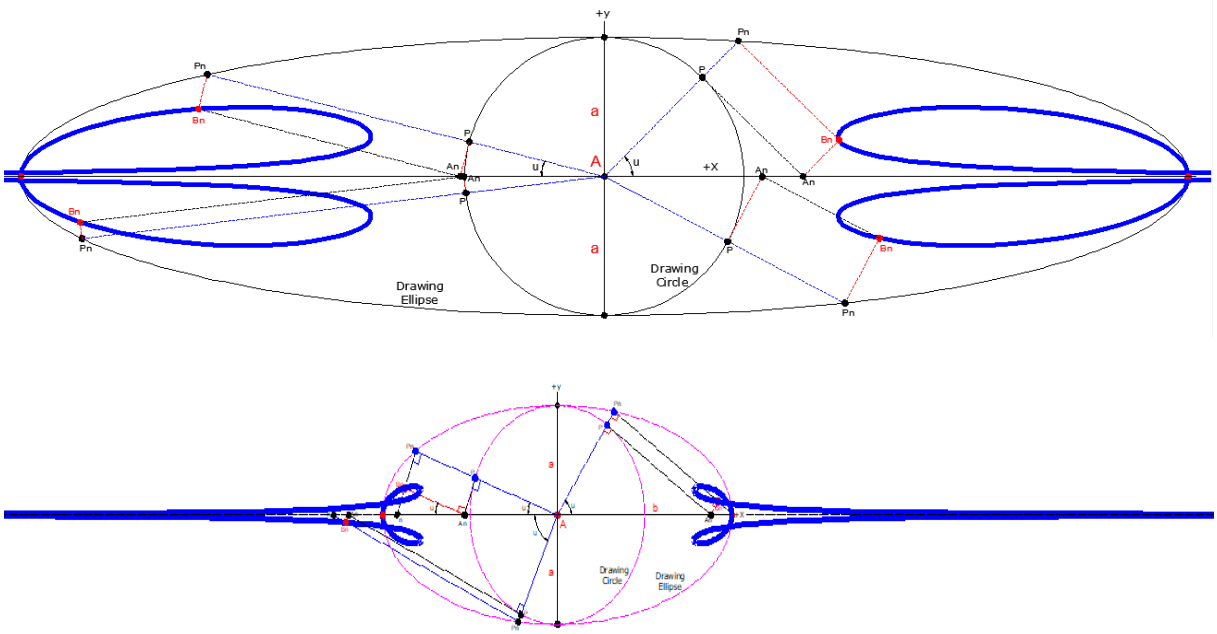

Picture 8. Plot the LBF's geometric properties (constructing method No.2), where the major axis is varied between (b = 2a) and (b = 3.25a).

Upon closely examining each point located along the x-axis of the ellipse, it becomes evident that the curves generate a couple of cusps that align themselves with a distinct auxiliary ellipse, as illustrated in Figure 8. Similarly, this method (No.2) phenomenon underscores the intricate relationship between the LBF's curve and these ancillary ellipses, suggesting the presence of deeper geometrical connections yet to be fully elucidated, Table 1.

Table 1 shows that each segment of the LBFs intersects the x-axis at a single point at a cusp ($\pm$ b, 0), while there is no point through which the LBFs reach the y-axis. Whenever the difference between the major and minor axis of the ellipse is increased, the shape of LBF's cusps gradually decreases; hence, the curve's cusp length and its shaded area simultaneously disappear whenever the difference value between a and b is bigger than 0.5b.

Table 1. The key elements of LBF's curve proportions.

Proportions	value
Start point.	$(\pm\infty, \pm\infty)$
Head point (Bn).	$(\pm 0.2334168b, \pm 0.29103239a)$
LBF's length (in infinity).	$\pm\infty$
LBF's length (inside the ellipse).	$3.14179256861940028b$
LBF's cusp area.	$4.54471760709808\ b^2$
Cusp's intersection point.	$(\pm b, 0)$
LBF's asymptotes.	The origin point (0,0)

Where (a) is the minor axis of the ellipse.
And (b) is the major axis of the ellipse

Discussions

The Kopper curve is studied in this article, and three special forms, LBF, are produced using two geometric methods. The mention of a particular construction method suggests a structured process that leads to the formation of the curve (Jin et al., 2021; Y. Lin et al., 2019; Rotmensch et al., 2017). The core assertion of the statement is that finite ranges do not bind the dual curves stemming from the LBF but instead perpetually extend in both the positive and negative directions along the x-axis. This infinite extension implies that the curve continues indefinitely without encountering any endpoint (method No.1); the *x*-axis, a fundamental reference line in Cartesian coordinates, plays a pivotal role in shaping the behavior of the LBF and its dual curves. The dual curves' extension along the x-axis implies that they persistently traverse in parallel to the x-axis, perpetually increasing or decreasing in magnitude as they proceed. The specific construction method referenced as "No.2" provides a delineated approach for generating a form of the LBF curve with dual cusps. The statement encapsulates that through a specific construction method (No.2), the LBF curve generates dual curves that possess the unique characteristic of infinite extension along the *x*-axis.

Significantly, an intriguing aspect of the duality of the LBF curve emerges when the radius of the circle (a) remains constant while the value of the major axis (b) of the drawing ellipse varies. This variation shows a noteworthy correlation between the nodes (cusps) of the LBF's curve and the associated ellipse. The profound implications of these geometric relationships necessitate additional scholarly investigation. The central question revolves around the potential of these curve configurations in shedding light on the geometric methodologies that underlie engineering processes, a domain that has historically garnered interest across various fields of study (Fioretos, 2011; Soutter et al., 2011; Zhang et al., 2019).

Conclusions and Suggestions

The diverse manifestations of LBF's curve represent a novel dual open curve derived from the combination of conic curvatures from a circle and an ellipse, complemented by parallel asymptotes. This article's resulting configuration demonstrates both boundless expansion and continuous behavior, unveiling an exceptional geometric property that beckons for more in-depth investigation and analysis. This condition implies that the geometric relationships associated with LBF's curve are intricate and multifaceted, necessitating further scrutiny. This initial proposition underscores our primary emphasis on exploring the geometric attributes of LBF's curve, thus indicating that the subsequent discussion will revolve around its structural characteristics and inherent behaviors. Therefore, these multifaceted geometrical complexities necessitate further exploration. Future inquiries have the capacity to reveal deeper insights into the exact nature of these geometric connections within the LBF curve. By venturing into these uncharted territories, subsequent academic endeavors may uncover a more comprehensive comprehension of the fundamental geometric principles that dictate the behavior of the LBF's curve. Hence, an appendix is dedicated to compiling additional instances of the LBF's curve, facilitating further investigation.

Acknowledgments

It gives immense pleasure to thank all those who extended their coordination, moral support, guidance, and encouragement to reach the publication of the article. My special thanks to my family, Angham S.M., Noor, Nada, Fatima, and Omneya, for their full support and coordination.

Author's declaration:

Conflicts of Interest: None.
I hereby confirm that all the Figures and Tables in the manuscript are mine. Besides, the Figures and images, which are not mine, have been permitted re-publication and attached to the manuscript.

References

Al-ossmi, L. H. M. (2023). An elementary treatise on elliptic functions as trigonometry. *Alifmatika: Jurnal Pendidikan Dan Pembelajaran Matematika*, *5*(1), 1–20. https://doi.org/10.35316/alifmatika.2023.v5i1.1-20

Bialy, M. (2022). Mather β-function for ellipses and rigidity. *Entropy*, *24*(11), 1600. https://doi.org/10.3390/e24111600

Bobenko, A. I., Schief, W. K., & Techter, J. (2020). Checkerboard incircular nets: Laguerre geometry and parametrisation. *Geometriae Dedicata*, *204*(1), 97–129. https://doi.org/10.1007/s10711-019-00449-x

Chan, M., Galatius, S., & Payne, S. (2021). Tropical curves, graph complexes, and top weight cohomology of $\mathcal{M}_{g}$. *Journal of the American Mathematical Society*, *34*(2),

565–594. https://doi.org/10.1090/jams/965

da Silva, J. L. E., da Silva, G. B., & Ramos, R. V. (2020). The lambert-kaniadakis wκ function. *Physics Letters A*, *384*(8), 126175. https://doi.org/10.1016/j.physleta.2019.126175

Findlen, P. (2011). Calculations of faith: mathematics, philosophy, and sanctity in 18th-century Italy (new work on Maria Gaetana Agnesi). *Historia Mathematica*, *38*(2), 248–291. https://doi.org/10.1016/j.hm.2010.05.003

Fioretos, O. (2011). Historical institutionalism in international relations. *International Organization*, *65*(2), 367–399. https://doi.org/10.1017/S0020818311000002

Ghuku, S., & Saha, K. N. (2019). A parametric study on geometrically nonlinear behavior of curved beams with single and double link rods, and supported on moving boundary. *International Journal of Mechanical Sciences*, *161*(1), 105065. https://doi.org/10.1016/j.ijmecsci.2019.105065

Gilani, S. M., Abazari, N., & Yayli, Y. (2020). Characterizations of dual curves and dual focal curves in dual Lorentzian space $ D^{3} _ {1} $. *Turkish Journal of Mathematics*, *44*(5), 1561–1577. https://doi.org/10.3906/mat-1909-6

Hašek, R. (2020). Exploration of dual curves using a dynamic geometry and computer algebra system. *Mathematics in Computer Science*, *14*(1), 391–398. https://doi.org/10.1007/s11786-019-00433-4

Jin, W., Derr, T., Wang, Y., Ma, Y., Liu, Z., & Tang, J. (2021). Node similarity preserving graph convolutional networks. *Proceedings of the 14th ACM International Conference on Web Search and Data Mining*, 148–156. https://doi.org/10.1145/3437963.3441735

Karkucinska-Wieckowska, A., Simoes, I. C. M., Kalinowski, P., Lebiedzinska-Arciszewska, M., Zieniewicz, K., Milkiewicz, P., Górska-Ponikowska, M., Pinton, P., Malik, A. N., & Krawczyk, M. (2022). Mitochondria, oxidative stress and nonalcoholic fatty liver disease: A complex relationship. *European Journal of Clinical Investigation*, *52*(3), 1–19. https://doi.org/10.1111/eci.13622

Lin, C.-C., & Yang, F.-L. (2018). A new image processing algorithm for three-dimensional angular velocity measurement and its application in a granular avalanche. *Advanced Powder Technology*, *29*(3), 506–517. https://doi.org/10.1016/j.apt.2018.02.004

Lin, Y., Sun, K., Liu, S., Chen, X., Cheng, Y., Cheong, W., Chen, Z., Zheng, L., Zhang, J., & Li, X. (2019). Construction of CoP/NiCoP nano tadpoles heterojunction interface for wide pH hydrogen evolution electrocatalysis and supercapacitor. *Advanced Energy Materials*, *9*(36), 1901213. https://doi.org/10.1002/aenm.201901213

Liu, T. (2017). *Ocular aberrations across the visual field during accommodation*. Indiana University. https://ui.adsabs.harvard.edu/abs/2017PhDT.....28L/abstract

Magnaghi-Delfino, P., & Norando, T. (2020). How to solve second-degree algebraic equations using geometry. *Faces of Geometry. From Agnesi to Mirzakhani*, 121–130. https://doi.org/10.1007/978-3-030-29796-1_11

Mary, H., & Brouhard, G. J. (2019). Kappa (κ): analysis of curvature in biological image data using B-splines. *BioRxiv*, 852772. https://doi.org/10.1101/852772

Miura, K. T., Gobithaasan, R. U., Salvi, P., Wang, D., Sekine, T., & Usuki, S. (2022). εκ-Curves: Controlled local curvature extrema. *The Visual Computer: International Journal of Computer Graphics*, *38*(1), 2723–2738. https://doi.org/10.1007/s00371-021-02149-8

Rotmensch, M., Halpern, Y., Tlimat, A., Horng, S., & Sontag, D. (2017). Learning a health knowledge graph from electronic medical records. *Scientific Reports*, *7*(1), 5994. https://doi.org/10.1038/s41598-017-05778-z

Saha, K. N. (2019). Evolving appropriate common engineering software: A case study. *Proceedings of International Academic Conferences*, *9110691*. https://ideas.repec.org/p/sek/iacpro/9110691.html

Simon Wedlund, C., Volwerk, M., Beth, A., Mazelle, C., Möstl, C., Halekas, J., Gruesbeck, J. R., & Rojas-Castillo, D. (2022). A fast bow shock location predictor-estimator from 2D and 3D analytical models: Application to mars and the maven mission. *Journal of Geophysical Research: Space Physics*, *127*(1), 1–31. https://doi.org/10.1029/2021JA029942

Soutter, A. K., Gilmore, A., & O'Steen, B. (2011). How do high school youths' educational experiences relate to well-being? Towards a trans-disciplinary conceptualization. *Journal of Happiness Studies*, *12*, 591–631. https://doi.org/10.1007/s10902-010-9219-5

Szubiakowski, J. P., & Włodarczyk, J. (2018). The solar dial in the olsztyn castle: its construction and relation to copernicus. *Journal for the History of Astronomy*, *49*(2), 158–195. https://doi.org/10.1177/0021828618776057

Usman, M., Abbas, M., & Miura, K. T. (2020). Some engineering applications of new trigonometric cubic Bézier-like curves to free-form complex curve modeling. *Journal of Advanced Mechanical Design, Systems, and Manufacturing*, *14*(4), 1–15. https://doi.org/10.1299/jamdsm.2020jamdsm0048

Wang, D., Gobithaasan, R. U., Sekine, T., Usuki, S., & Miura, K. T. (2021). *Interpolation of point sequences with extremum of curvature by log-aesthetic curves with G2 continuity*. https://www.cad-journal.net/files/vol_18/CAD_18(2)_2021_399-410.pdf

Weil, A. B., Gutiérrez-Alonso, G., Johnston, S. T., & Pastor-Galán, D. (2013). Kinematic constraints on buckling a lithospheric-scale orocline along the northern margin of gondwana: A geologic synthesis. *Tectonophysics*, *582*, 25–49. https://doi.org/10.1016/j.tecto.2012.10.006

Więckowska, B., Kubiak, K. B., Jóźwiak, P., Moryson, W., & Stawińska-Witoszyńska, B. (2022). Cohen's kappa coefficient as a measure to assess classification improvement following the addition of a new marker to a regression model. *International Journal of Environmental Research and Public Health*, *19*(16), 10213. https://doi.org/10.3390/ijerph191610213

Yan, Z., Schiller, S., & Schaefer, S. (2019). Circle reproduction with interpolatory curves at local maximal curvature points. *Computer Aided Geometric Design*, *72*, 98–110. https://doi.org/10.1016/j.cagd.2019.06.002

Yücesan, A., & Tükel, G. Ö. (2020). A new characterization of dual general helices. *4th International Conference On Mathematics*. https://www.researchgate.net/publication/348325667_A_New_Characterization_of_Dual_General_Helices

Zhang, S., Yao, L., Sun, A., & Tay, Y. (2019). Deep learning based recommender system: A survey and new perspectives. *ACM Computing Surveys (CSUR)*, *52*(1), 1–38. https://doi.org/10.1145/3285029

Attachment

Appendix (A): a set of special cases of LBF's curve.

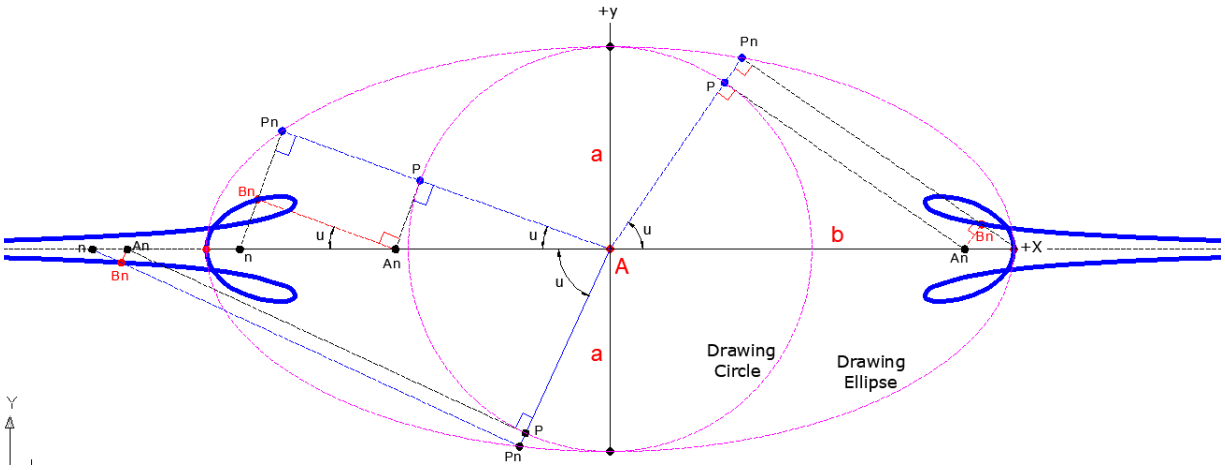

Picture 1. The LBF's curve with cusps, when ($PnBn = PAn$)

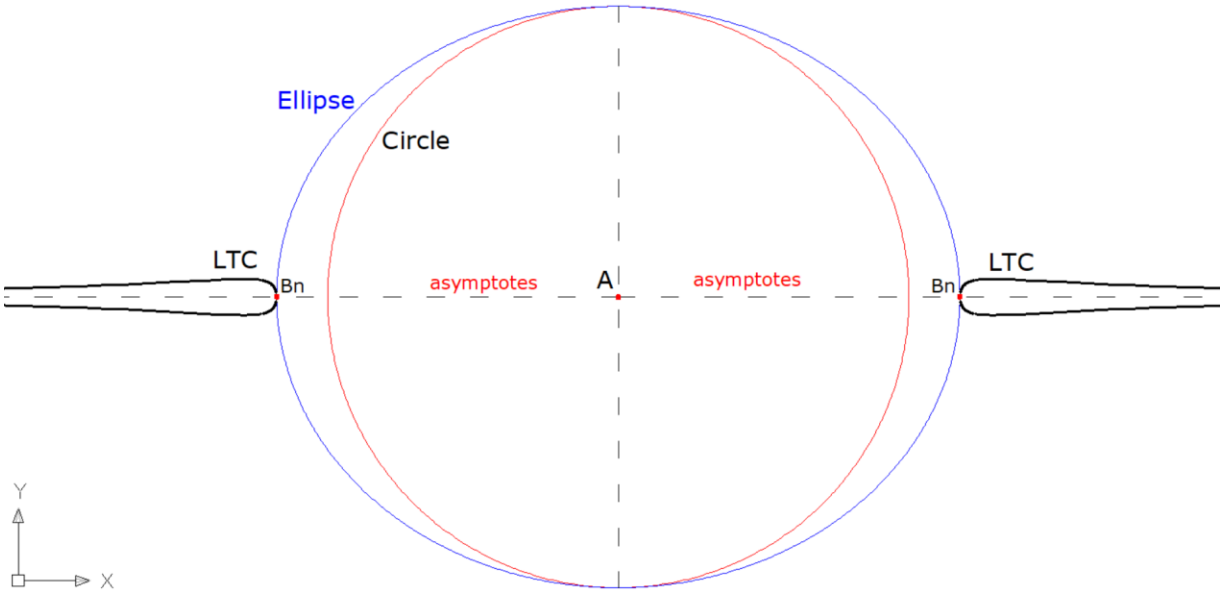

Picture 2. Plot the LBF's curve without cusps when ($b = 1.17539a$)

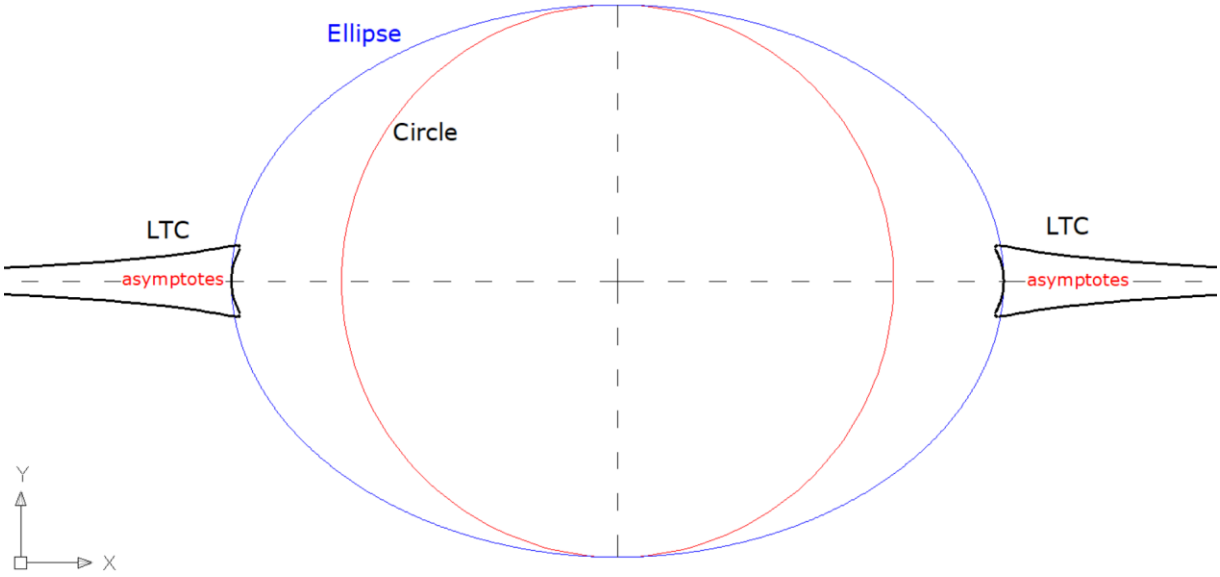

Picture 3. Plot the LBF's curve with cusps when (b = 1.39869a)

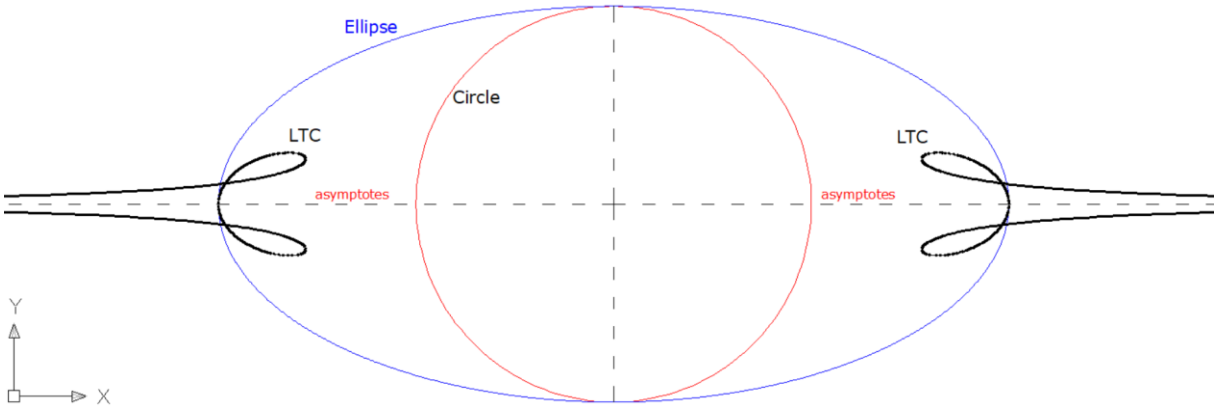

Picture 4. Plot the LBF's curve with cusps when (b = 2.00a)

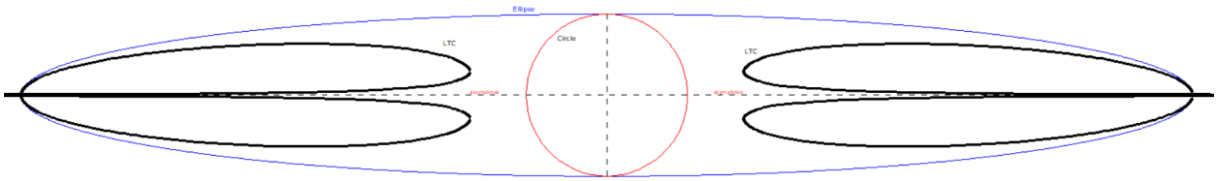

Picture 5. Plot the LBF's curve with cusps when (b = 7.267a)

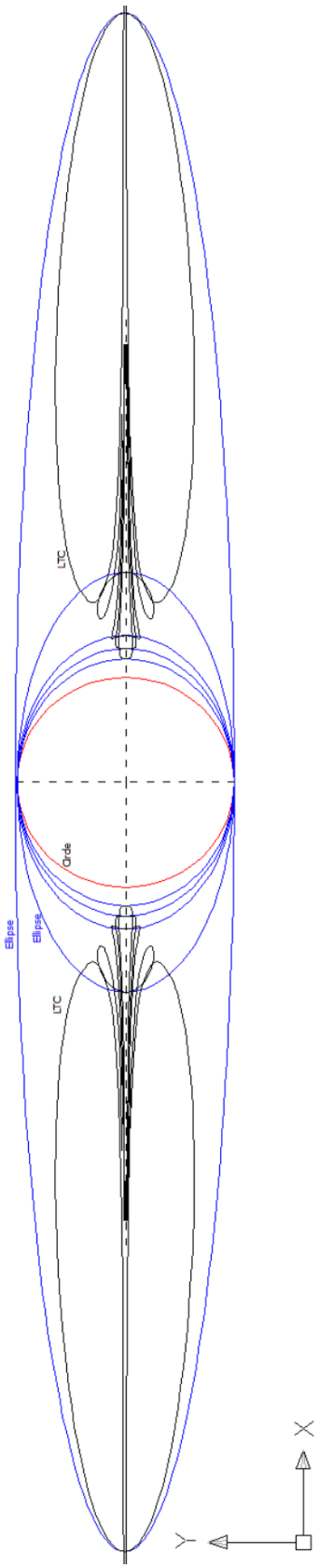

Picture 6. Plot the LBF's curve by 5 cases, where a is fixed while b is varied from; (1.17539a), (1.39869a), (2.00a), and (7.267a).